Building and Environment 274 (2025) 112651

Contents lists available at ScienceDirect

Building and Environment

journal homepage: www.elsevier.com/locate/buildenv

Spatiotemporal variations in ozone and carbon dioxide concentrations in an HVAC system of a LEED-certified office building

Jinglin Jiang, Junkai Huang, Nusrat Jung, Brandon E. Boor *

Lyles School of Civil and Construction Engineering, Purdue University, West Lafayette, IN 47907, United States

A R T I C L E I N F O

Keywords:
Indoor air quality
Building ventilation
Indoor chemistry
Occupancy
Ozone dynamics

A B S T R A C T

Indoor air quality (IAQ) is crucial for the health, well-being, and productivity of office occupants. IAQ is strongly influenced by occupancy and the operational mode of the heating, ventilation, and air conditioning (HVAC) system. This study investigates the spatiotemporal variations in ozone (O_3) and carbon dioxide (CO_2) concentrations throughout the HVAC system of a LEED-certified office building. A four-month field measurement campaign was conducted at the Ray W. Herrick Laboratories, employing an automated multi-point sampling system to monitor O_3 and CO_2 at eight locations throughout the HVAC system. The objectives of this study are to characterize the spatiotemporal distribution of these gases under different ventilation modes and occupancy levels, and to identify O_3 loss mechanisms in the office and its HVAC system. Spatiotemporal variations in O_3 and CO_2 concentrations were observed throughout the HVAC system. Results indicate that outdoor air exchange rates (AERs) significantly impact indoor O_3 levels, with higher AERs resulting in increased indoor O_3 but reduced CO_2 concentrations. Measurements reveal that HVAC filters and ducts contribute to O_3 loss, with up to 18% O_3 removal observed in the longest HVAC duct segment. Additionally, occupancy influences O_3 deposition onto human skin and clothing surfaces. This research underscores the limitations of ventilation standards that focus only on CO_2, highlighting the need for ventilation strategies that consider the effects of occupancy and outdoor AERs on different gases. By integrating multi-point gas sampling into building automation systems, more effective control strategies can be developed to enhance IAQ and occupant health while reducing energy consumption.

1. Introduction

Indoor air quality (IAQ) in office buildings can impact the health, well-being, and productivity of the occupants [1–3]. Operation of building heating, ventilation, and air conditioning (HVAC) systems and occupant activities are two important factors that may affect the dynamics and chemistry of indoor air pollutants, including airborne particles, volatile organic compounds (VOCs), nitrogen oxides (NO_x: NO and NO_2), ozone (O_3), and carbon dioxide (CO_2). Among these indoor air pollutants, O_3 and CO_2 are two important trace gases that are strongly connected to IAQ. In most buildings, especially in office buildings without combustion sources, the exhaled breath of occupants is the major source of CO_2 [4,5]. O_3 is an important driver of indoor oxidative reactive chemistry. O_3 can react with VOCs such as monoterpenes emitted by human activities, including cleaning and disinfecting surfaces, and initiate the formation of secondary organic aerosol (SOA) [6–11]. In addition, O_3 can react with compounds on indoor surfaces including building surfaces and human body surfaces. O_3 reacts with unsaturated compounds in human skin oil, including squalene, glycerides, fatty acids, and cholesterols, leading to the formation of volatile skin oil ozonolysis products and SOA [12–16]. O_3-skin oil reactions are considered one of the major O_3 sinks in occupied indoor environments [12]. Both O_3 itself and its secondary reaction products can have adverse effects on human health. Human exposure to O_3 has been associated with respiratory and cardiovascular morbidity and mortality [17–21]. 4-oxopentanal (4-OPA), a reaction product of O_3 and skin oil, can cause irritation of the respiratory system and skin [22–25].

LEED-certified office buildings often implement sophisticated HVAC systems with building automation systems to control parameters related to the indoor thermal environment and IAQ, while minimizing energy consumption. Mixing ratios of indoor CO_2 are strongly associated with the design and operation of mechanical ventilation systems [26–29]. Outdoor and exhaust volumetric airflow rates determine the air exchange rate (AER) of the building, which directly impacts CO_2 loss and

* Corresponding author.
E-mail address: bboor@purdue.edu (B.E. Boor).

https://doi.org/10.1016/j.buildenv.2025.112651
Received 4 July 2024; Received in revised form 10 December 2024; Accepted 28 January 2025
Available online 29 January 2025

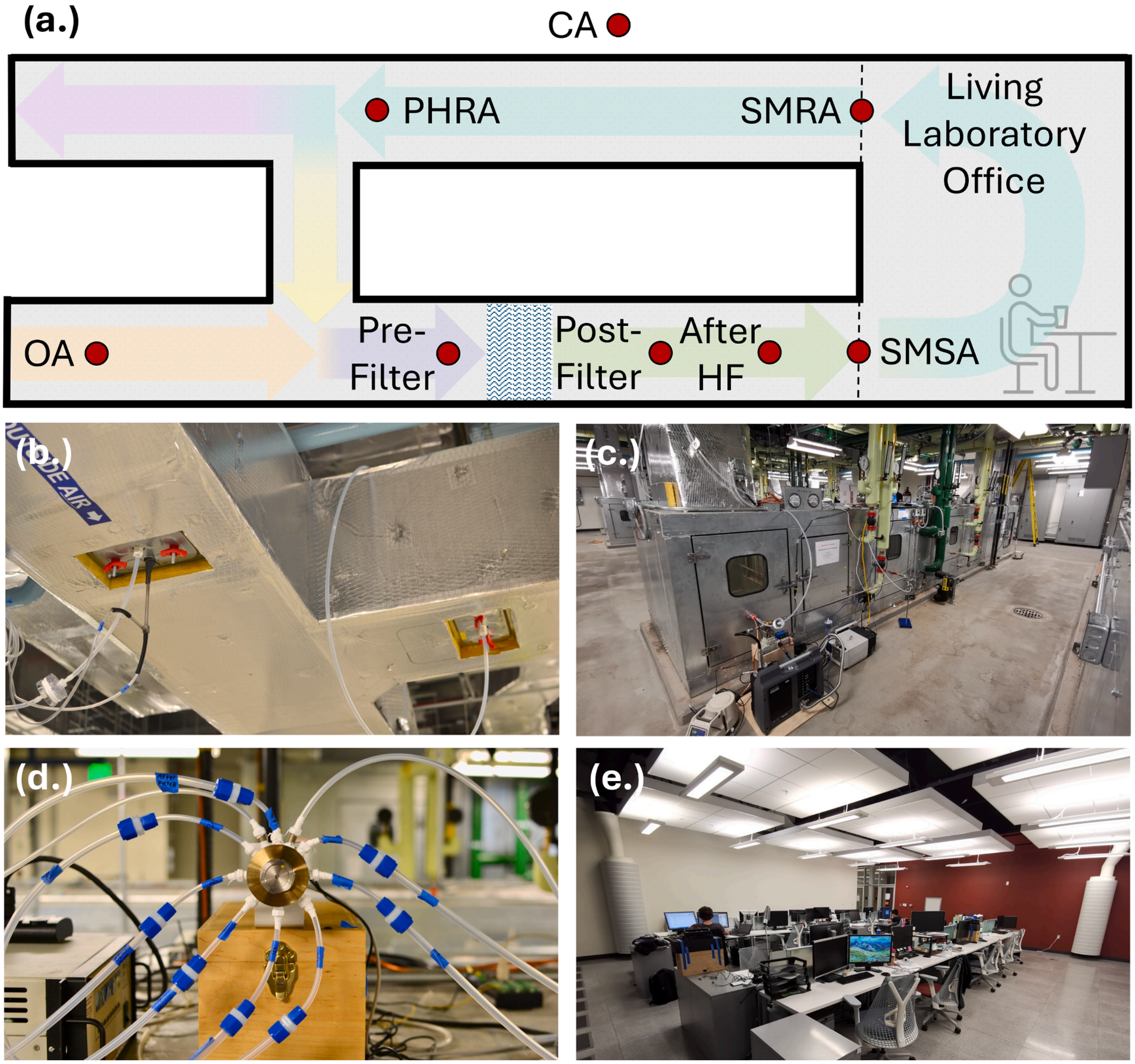

Fig. 1. (a.) Schematic of the experimental setup for multi-point sampling of O_3 and CO_2 mixing ratios throughout the HVAC system of the living laboratory office. The eight sampling locations are noted in the schematic and include: the outdoor air intake (OA), upstream of the HVAC filter bank (Pre-Filter), downstream of the HVAC filter bank (Post-Filter), after the steam humidifier (After HF), supply air duct located in the small mechanical room (SMSA), return air duct located in the small mechanical room (SMRA), return air duct located in the penthouse (PHRA), and the common area (CA) adjacent to the office; (b.) photo of the OA and PHRA sampling locations in the penthouse; (c.) photo of the Pre-Filter and Post-Filter sampling locations from the HVAC system; (d.) photo of the programmable multi-flow path selector connected to the O_3 and CO_2 gas analyzers; and (e.) photo of the living laboratory office.

CO_2 mixing ratios in buildings. CO_2 mixing ratios are commonly monitored in building automation systems as an indicator of ventilation conditions, occupancy levels, or other indoor air pollutants [30–32]. ANSI/ASHRAE Standard 62.1–2022 has been established to regulate the minimum outdoor volumetric airflow rate in buildings based on the number of people present or the area of the office space [33]. However, most standards primarily focus on CO_2 levels and do not adequately address the complexities of IAQ, such as the presence and dynamics of other critical air pollutants like O_3. This limitation can lead to ventilation strategies that fail to comprehensively protect occupant health and well-being.

A building's mechanical ventilation system may impact indoor O_3 mixing ratios and dynamics differently than that for CO_2, which is an inert gas. Ventilation systems are the major pathway for outdoor O_3 to enter indoor environments [34–36], which could further impact indoor oxidative reactive chemistry and the formation of secondary gas- and particle-phase products. In addition, the surfaces of HVAC ducts and the components of HVAC systems, including the HVAC filter bank and heating and cooling coils, could be a sink for outdoor O_3 as it is transported through the HVAC ducts before being supplied to the office [37–39]. However, current common HVAC system control strategies for IAQ are predominantly based on CO_2 sensing or modeling [40–43]. Furthermore, very few systems monitor trace gas concentrations at multiple locations within the HVAC system, failing to account for the impact of HVAC ducts and the operational conditions of HVAC components on IAQ in their control logic. Simultaneous real-time monitoring of the mixing ratios of these trace gases throughout building HVAC systems is critical to improve our understanding on indoor air pollutant dynamics and chemistry, providing data and information to determine appropriate ventilation strategies that improve IAQ.

However, to the authors' knowledge, there have been no prior long-term, multi-location measurements of O_3 and CO_2 throughout a commercial HVAC system under different ventilation and occupancy conditions. This study proposes and presents a novel automated multi-location sampling system that has a wide range of applications, especially for ventilation control and improving IAQ. Specifically, this study investigates how the HVAC system operational mode and occupancy impact the spatiotemporal distribution of O_3 and CO_2 mixing ratios, as well as O_3 dynamics, in a ventilation system of a LEED-certified office building. A four-month field measurement campaign was conducted from February to June 2019 in one of the four occupied open-plan living laboratory offices at the Purdue University Ray W. Herrick Laboratories, which was awarded a LEED Gold Certificate. An automated multi-point sampling system was designed and built to monitor O_3 and CO_2 mixing ratios throughout the HVAC system in real-time. The objectives of this study are: (1.) to characterize the spatiotemporal distribution of O_3 and CO_2 mixing ratios at eight different sampling locations throughout the ventilation system of the office building under different HVAC system operational modes, including outdoor AERs and pressurization conditions, and different occupancy levels; (2.) to understand how the indoor/outdoor (I/O) ratio of O_3 and CO_2 mixing ratios are related to the operational mode of the mechanical ventilation system and human occupancy levels; and (3.) to understand loss mechanisms for O_3 in the office and throughout its HVAC system.

2. Materials and methods

2.1. Site description: Herrick living laboratory open-plan offices at Purdue University

The study site, one of the four Herrick living laboratory offices, is part of a LEED-certified building at Purdue University in West Lafayette, IN, U.S. (40°25′19.4″N 86°55′11.6″W). The living laboratories are four reconfigurable, side-by-side large open-plan office spaces, with a maximum occupancy of 20 and interior volume of 333 m^3. Each office includes its own HVAC system, which is equipped with a MERV-8 pre-filter and a MERV-14 final-filter (Fig. 1). A building automation system (Niagara/AX, Tridium Inc., Richmond, VA, U.S.), along with hundreds of sensors, is applied to achieve real-time monitoring and precise control of the HVAC system. These sensors monitor air temperatures, relative humidities, volumetric airflow rates, damper positions, and fan speeds at different locations throughout the HVAC system; this provides a detailed airflow profile for the entire system. Damper positions and fan speeds were changed throughout the campaign to adjust the supply, return, and outdoor volumetric airflow rates.

2.2. Experimental setup and air quality instrumentation

2.2.1. Automated multi-point sampling system for the monitoring of O_3 and CO_2 mixing ratios

An automated multi-point sampling system was built with a programmable multi-flow path selector (EUTA-2VLSC8MWE2, Valco Instruments Co. Inc., Houston, TX, U.S.) to sample O_3 and CO_2, as well as NO_x and VOCs, at eight locations throughout the HVAC system (Fig. 1). The sampling locations included: the outdoor air intake (OA), upstream of the HVAC filter bank (Pre-Filter), downstream of the HVAC filter bank (Post-Filter), after the steam humidifier (After HF), supply air duct located in the small mechanical room (SMSA), return air duct located in the small mechanical room (SMRA), return air duct located in the penthouse (PHRA), and the common area (CA) adjacent to the living laboratory office (Fig. 1). Perfluoroalkoxy (PFA) tubing (3/8″ (9.5 mm) OD) was used for the sampling lines to connect each sampling location to the multi-flow path selector. The selected flow path outlet was connected to trace gas analyzers. The unselected streams were purged by a rough pump to prevent accumulation of stagnant air in the lines. This was done to eliminate a time delay in sampling. The total flow rate of the selected stream was maintained at 11.25 L min^{-1} with a vacuum pump drawing the sample air at 9 L min^{-1}. This ensured that the residence time of the sample air was no more than 8 s. A polytetrafluoroethylene (PTFE) membrane filter was installed at the inlet of each sampling line to remove particles and was replaced daily to ensure its efficacy.

Table 1
Multi-point sampling sequences implemented during the field measurement campaign.

Sequence	Multi-Point Sampling Sequence
Spatial	4 min outdoor air (OA) + 4 min Pre-Filter + 4 min Post-Filter + 4 min after humidifier (After HF) + 4 min supply air (SMSA) + 4 min return air (SMRA) + 3 min return air (PHRA) + 3 min common area (CA)
Temporal	5 min outdoor air (OA) + 5 min supply air (SMSA) + 20 min return air (SMRA)
Pre-/Post-Filter	4 min Pre-Filter + 4 min Post-Filter

2.2.2. Instrumentation for the real-time monitoring of O_3 and CO_2 mixing ratios and office occupancy

An O_3 gas analyzer (Model M400E, Teledyne Technologies Inc., Thousand Oaks, CA, U.S.) and a CO_2 gas analyzer (LI-830, LI-COR Biosciences, Lincoln, NE, U.S.) were connected to the selected flow path outlet of the multi-flow path selector to alternatively monitor O_3 and CO_2 mixing ratios at the eight locations in real-time (1 Hz). The CO_2 analyzer was operated at a flow rate of 0.75 L min^{-1}. The O_3 gas analyzer monitored O_3 mixing ratios with a precision of 1 ppb using a photometric analyzer based on ultraviolet absorption of O_3 at 254 nm, with a sample flow rate at 0.8 L min^{-1}. Nitrogen oxides (NO and NO_2) were measured by a chemiluminescence NO-NO_2-NO_x analyzer (Model 42C, Thermo Electron Corp., Waltham, MA, U.S.) with a sample flow rate at 0.6 L min^{-1}. VOCs with a proton affinity greater than water were monitored by a proton transfer reaction time-of-flight mass spectrometer (PTR-TOF-MS, PTR-TOF 4000, Ionicon Analytik Ges.m.b.H., Innsbruck, Austria) using H_3O^+ as the reagent ion. The inlet flow rate was maintained at 0.1 L min^{-1}. Details of the PTR-TOF-MS measurements can be found in Wu et al. (2021 and 2024) [44,45]. The O_3, CO_2, and NO-NO_2-NO_x analyzers were calibrated before the measurement campaign. The PTR-TOF-MS was calibrated daily following protocols described in previous studies [6,45–49]. Human occupancy in the living laboratory was tracked via chair-embedded thermocouples during the measurement campaign as described in Wagner et al. (2021) [50].

2.2.3. Multi-point sampling system sequences

During the measurement campaign, three different sequences for the multi-point sampling system were implemented. (1.) Sequence 1: a 30 min spatial sequence. The spatial sequence was designed to monitor spatial variations in O_3 and CO_2 mixing ratios across the eight locations of the HVAC system, which can inform how different HVAC components impact O_3 chemistry. During the spatial sequence, the valve system switched to OA, Pre-Filter, Post-Filter, After HF, SMSA, and SMRA for 4 min each, then PHRA and CA for 3 min each. (2.) Sequence 2: a 30 min temporal sequence, which specifically focused on O_3 and CO_2 dynamics in the office. This enabled for a more detailed investigation into the impact of occupants and ventilation conditions on indoor O_3 and CO_2 mixing ratios. During the temporal sequence, SMRA was sampled for 20 min, and then SMSA and OA were sampled for 5 min each. (3.) Sequence 3: an 8 min pre-/post-filter sequence. To investigate the role of the HVAC filter bank on O_3 dynamics, a pre-/post-filter sequence was designed to sample only the pre-filter and post-filter locations with 4 min of sampling at Pre-Filter and 4 min of sampling at Post-Filter. Details of each valve sequence are provided in Table 1. The O_3 and CO_2 mixing ratios for each location presented in the results are the mean values during the 30-min sample sequence for sequences 1 and 2. The first minute and last minute of data at each sampling location was disregarded to avoid the impact of the valve switching. For the pre-/post-filter sequence, data when the valve was sampling from another location was interpolated to better compare the difference in O_3 mixing ratios upstream and downstream of the HVAC filter bank.

Table 2
Ventilation modes and their corresponding outdoor AERs and office pressurization conditions.

Ventilation Mode	Outdoor AER	Office Pressurization
1	Low	No
2	Medium	No
3	High	No
4	Low	Yes
5	Medium	Yes
6	High	Yes
7	Natural Ventilation	–

2.2.4. HVAC system operational modes during the measurement campaign

To investigate how the operation of the HVAC system impacts indoor O_3 and CO_2 dynamics, the supply, return, and outdoor volumetric airflow rates were adjusted to achieve different outdoor AERs and room pressurization conditions under different ventilation modes. The ratio of the recirculation airflow rate to the total supply airflow rate was adjusted from 0 to 1 to achieve different AERs. Throughout the campaign, based on the AERs and pressurization conditions, the ventilation modes can be categorized as follows: (1.) Mode 1: low AER ($\leq$ 2.7 h^{-1}), no pressurization; (2.) Mode 2: medium AER (2.7 h^{-1} < AER $\leq$ 5.4 h^{-1}), no pressurization; (3.) Mode 3: high AER (> 5.4 h^{-1}), no pressurization; (4.) Mode 4: low AER, pressurization; (5.) Mode 5: medium AER, pressurization; (6.) Mode 6: high AER, pressurization; and (7.) Mode 7: natural ventilation with unfiltered outdoor air via a south-facing, full-size double-skin glass façade. Table 2 summarizes the ventilation modes implemented during the campaign. The corresponding dates for each ventilation mode are summarized in a calendar in Fig. 2.

2.3. Material balance model to characterize O_3 loss terms in the office

To quantify the dynamics of O_3 in the living laboratory office, a simplified material balance model was developed to estimate the overall loss rate for O_3 under different ventilation and occupancy conditions:

$$\frac{dC_i(t)}{dt} = p\lambda_{in}(t)C_o(t) + \frac{C_o(t)Q_o(t)}{V} - L(t)C_i(t) \tag{1}$$

where $C_i(t)$ is the indoor O_3 mixing ratio (ppb) sampled at SMRA; p is the penetration factor for O_3 (-); $\lambda_{in}(t)$ is the infiltration rate (h^{-1}); $C_o(t)$ is the outdoor O_3 mixing ratio (ppb) sampled at OA; $Q_o(t)$ is the outdoor air volumetric airflow rate (m^3 h^{-1}); V is the volume of the living laboratory office (m^3); and $L(t)$ is the overall O_3 loss rate (h^{-1}). The office was treated as a completely mixed flow reactor (CMFR). There were no obvious indoor O_3 sources in the office, such as photocopiers or air purifiers, thus, an indoor emission term for O_3 is not included in the material balance model.

The time-dependent overall loss rate $L(t)$ for O_3 can be estimated by rearranging Eq. (1) as follows:

$$L(t) = -\frac{\frac{C_i(t+dt) - C_i(t)}{dt} - p\lambda_{in}(t)C_o(t) - \frac{C_o(t)Q_o(t)}{V}}{C_i(t)} \tag{2}$$

For a 30 min spatial sequence or a 30 min temporal sequence, the time interval was defined as: $dt = 30\ min$. The mean SMRA and OA O_3 mixing ratios during the 30 min period were taken as the values for $C_i(t)$ and $C_o(t)$, respectively. Similarly, the mean value of the outdoor air volumetric airflow rate during the 30 min period was taken as the value for $Q_o(t)$.

The overall loss rate for O_3 includes indoor O_3 removal by exfiltration, deposition to building surfaces and human body surfaces, building ventilation (outdoor air exchange), and gas-phase reactions with indoor NO_x and selected VOCs, as shown in Eq. (3):

$$L(t) = \lambda_{ex}(t) + \frac{v_{d,bldg}S_{bldg}}{V} + \frac{v_{d,occ}(t)S_{occ}(t)}{V} + \frac{Q_o(t)}{V} + L_{reaction}(t) \tag{3}$$

where $\lambda_{ex}(t)$ is the exfiltration rate (h^{-1}); $v_{d,bldg}$ is the O_3 deposition velocity to interior building material surfaces in the office (m h^{-1}); S_{bldg} is the surface area of interior building material surfaces in the office, assumed to be constant over time (m^2); $v_{d,occ}(t)$ is the O_3 deposition velocity to office occupant surfaces (m h^{-1}); $S_{occ}(t)$ is the surface area of

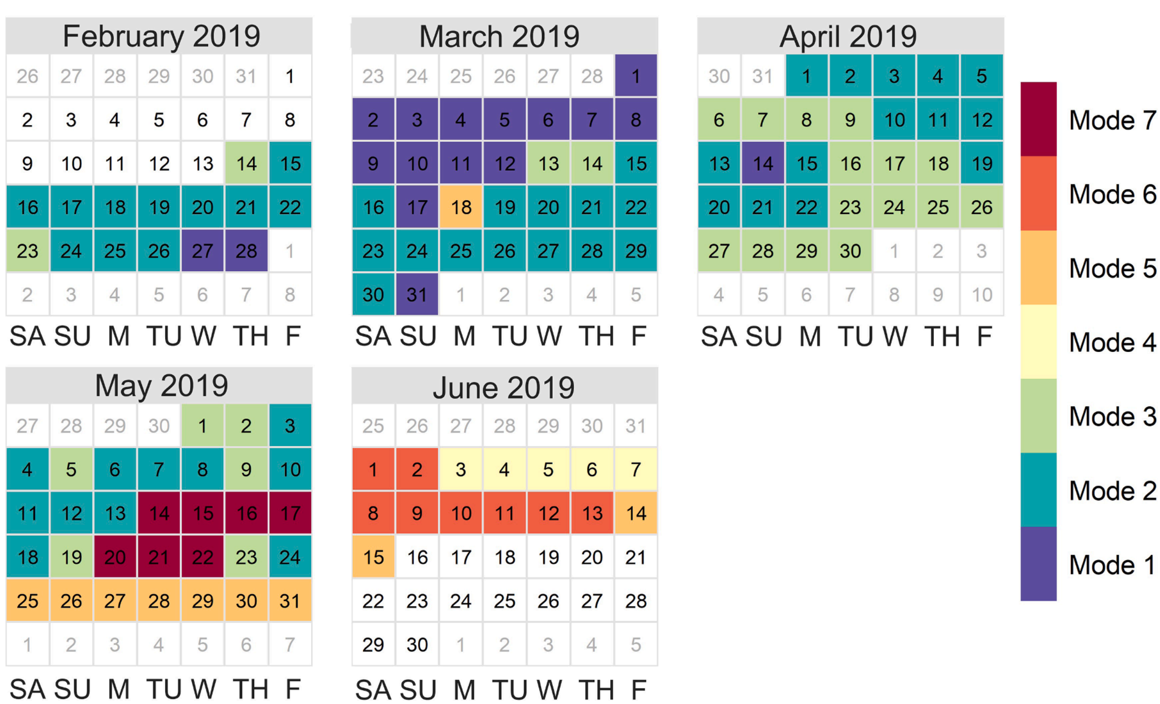

Fig. 2. Ventilation modes implemented throughout the four-month measurement campaign, including: (1.) Mode 1: low AER ($\leq$ 2.7 h^{-1}), no pressurization; (2.) Mode 2: medium AER (2.7 h^{-1} < AER $\leq$ 5.4 h^{-1}), no pressurization; (3.) Mode 3: high AER (> 5.4 h^{-1}), no pressurization; (4.) Mode 4: low AER, pressurization; (5.) Mode 5: medium AER, pressurization; (6.) Mode 6: high AER, pressurization; and (7.) Mode 7: natural ventilation with unfiltered outdoor air.

Table 3
Reaction rate constants of O_3 reactions with various gas-phase compounds.

Chemical Formula	Compound Name	Reaction Rate Constant (cm^3 molecule^{-1} s^{-1})	Indoor Concentration Range (ppb)
C_4H_8	1-Butene	1.00E-17 [52]	0 – 10
C_5H_8	Isoprene	1.28E-17 [52]	0 – 2
$C_{10}H_{16}$	Limonene	2.08E-16 [51]	0 – 10
NO	Nitrogen monoxide	1.40E-12 [53]	0 – 1
NO_2	Nitrogen dioxide	3.50E-17 [53]	0 – 2.5

the office occupants, which varies with the occupancy in the office (m^2); and $L_{reaction}(t)$ is the loss rate due to O_3 reactions with indoor NO_x and selected VOCs, including butene (C_4H_8), isoprene (C_5H_8), and monoterpenes ($C_{10}H_{16}$) (h^{-1}). $L_{reaction}(t)$ can be expressed as:

$$L_{reaction}(t) = \sum_i k_i[M_i(t)] \tag{4}$$

where $[M_i(t)]$ is the concentration of compound M_i (molecule cm^{-3}) and k_i is the reaction rate constant of the reaction between O_3 and compound M_i (cm^3 molecule^{-1} s^{-1}). Limonene and isoprene, two VOCs associated with human-related emissions, and NO_x, with outdoor air as the major source, were considered for O_3 reactions. 1-Butene, with relatively high concentrations observed during the campaign and a relatively high reaction rate with O_3, was considered as well. Their corresponding reaction rate constants and range of concentrations are summarized in Table 3. The reaction rate constants were obtained from the National Institute of Standards and Technology (NIST) Chemical Kinetics Database [51–54]. An average deposition velocity to interior building material surfaces in the office of $v_{d,bldg} = 1.62$ m h^{-1} was applied throughout the loss rate calculation. With all other parameters known, the O_3 deposition velocity to human body surfaces, $v_{d,occ}(t)$, can be back calculated with the assumption that the surface area of each occupant is approximately 1.7 m^2 [55].

The loss mechanisms of indoor O_3 listed above contribute to the difference between indoor and outdoor O_3 mixing ratios, which can be described by the "O_3 loss" ($C_{loss}(t)$). O_3 loss is a metric to evaluate the adverse health effects from human exposure to oxidation products from O_3 reactions and separate them from exposures to indoor O_3 itself [56]. The O_3 loss can be expressed as:

$$C_{loss}(t) = C_o(t) - C_i(t) \tag{5}$$

3. Results and discussion

3.1. Spatiotemporal variations in O_3 and CO_2 mixing ratios throughout the HVAC system

The diurnal trends of O_3 and CO_2 mixing ratios at the seven sampling locations (CA not shown) throughout the HVAC system under the three

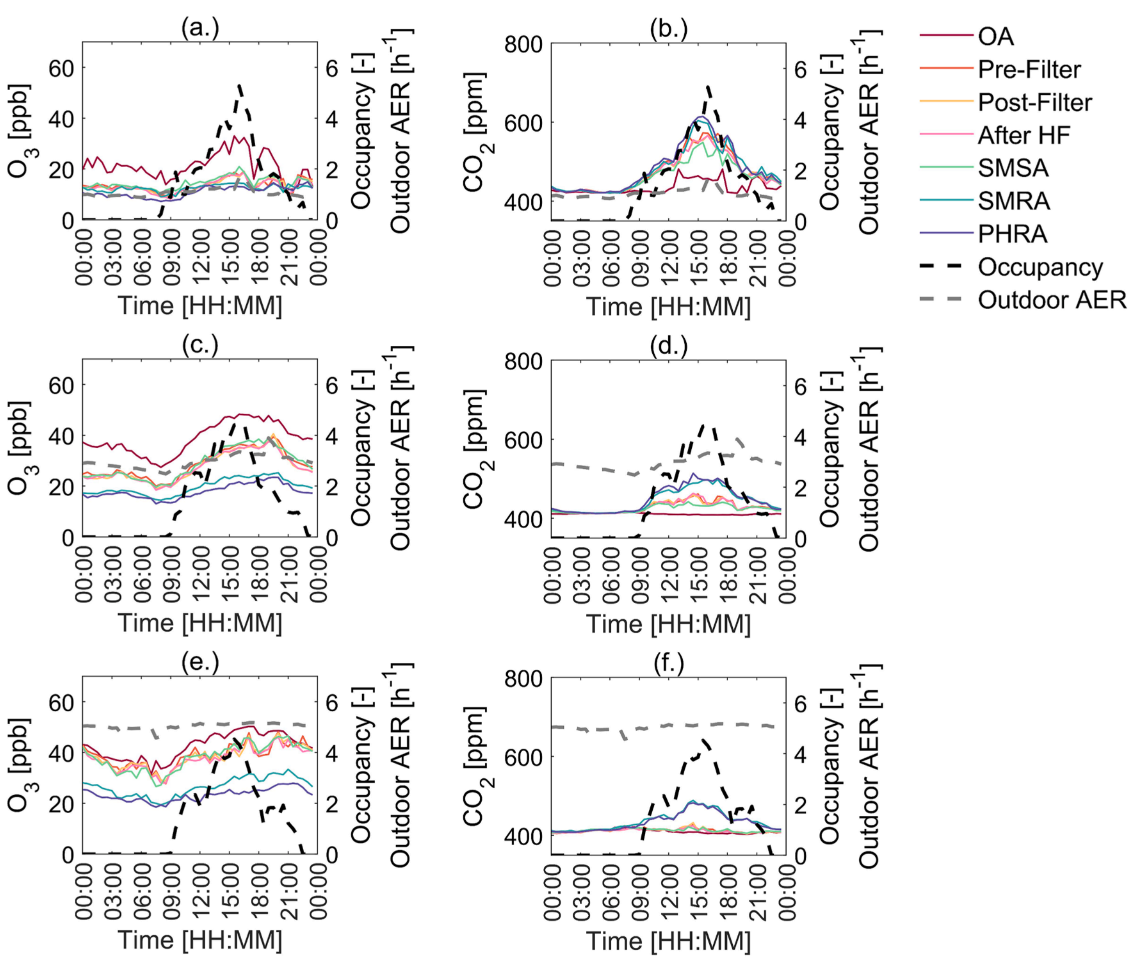

Fig. 3. Diurnal trends of (a.) O_3 and (b.) CO_2 mixing ratios under ventilation mode 1: low AER, no pressurization; (c.) O_3 and (d.) CO_2 mixing ratios under ventilation mode 2: medium AER, no pressurization; (e.) O_3 and (f.) CO_2 mixing ratios under ventilation mode 3: high AER, no pressurization. Occupancy (black dashed line) and outdoor AER (gray dashed line) are plotted on the right axis. The O_3 and CO_2 mixing ratios, outdoor AER, and occupancy are the median values of all days under the same ventilation mode category.

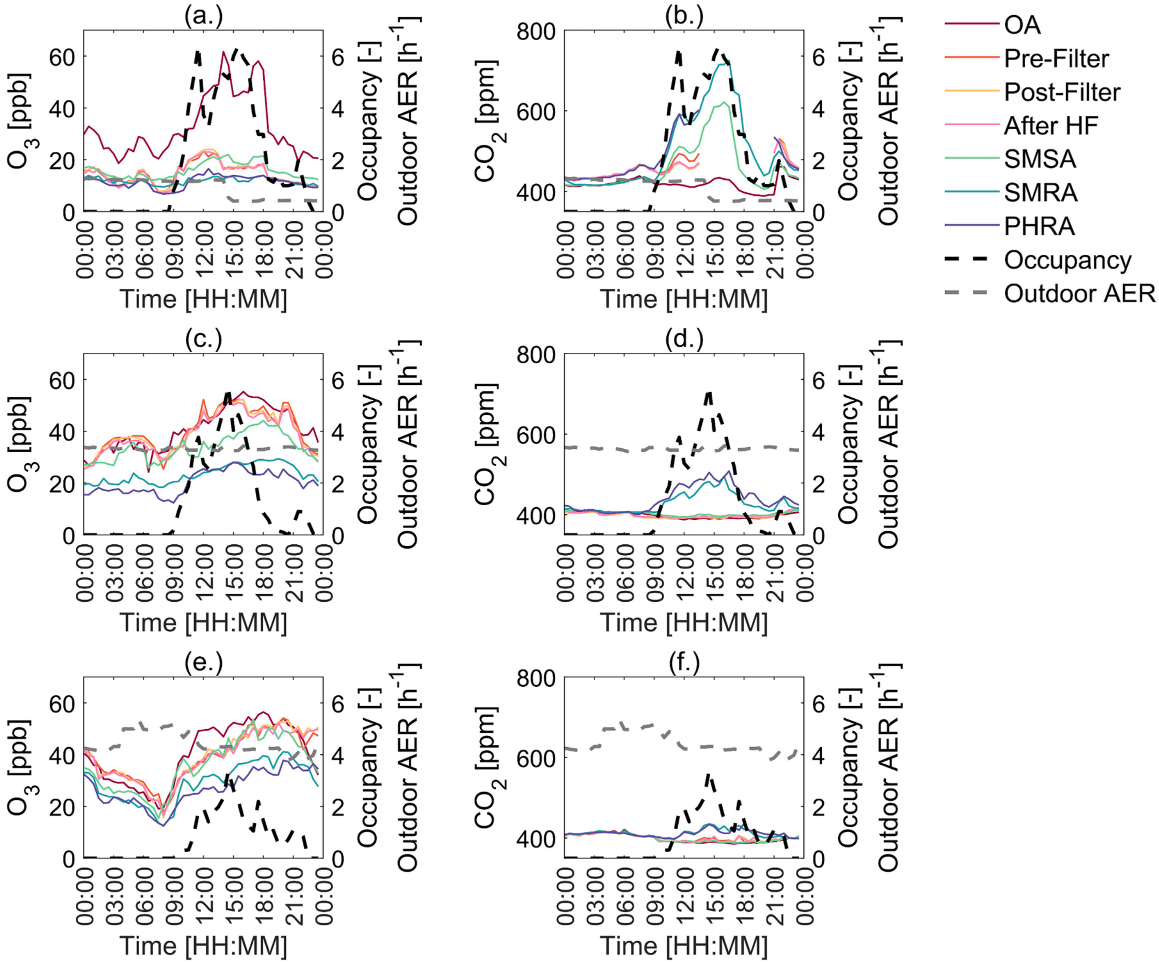

Fig. 4. Diurnal trends of (a.) O_3 and (b.) CO_2 mixing ratios under ventilation mode 4: low AER, pressurization; (c.) O_3 and (d.) CO_2 mixing ratios under ventilation mode 5: medium AER, pressurization; (e.) O_3 and (f.) CO_2 mixing ratios under ventilation mode 6: high AER, pressurization. Occupancy (black dashed line) and outdoor AER (gray dashed line) are plotted on the right axis. The O_3 and CO_2 mixing ratios, outdoor AER, and occupancy are the median values of all days under the same ventilation mode category.

non-pressurized ventilation operational modes 1 to 3 are presented in Fig. 3. O_3 mixing ratios at OA started increasing gradually at around 08:00 in the morning and peaked in the afternoon at around 17:00, which is consistent with previous observations of diurnal trends in outdoor O_3 mixing ratios [57–59]. Under ventilation modes 1 to 3 with low, medium, and high outdoor AERs, the SMRA O_3 mixing ratios peaked at 14, 25, and 33 ppb, respectively. As outdoor O_3 introduced via mechanical ventilation is the major source of indoor O_3 for this office, the outdoor AER has a strong impact on indoor O_3 mixing ratios. The SMRA CO_2 mixing ratio peaked at 15:00 to 16:00 in the afternoon, following the trend of the human occupancy level in the office. For example, as shown in Fig. 3(b.), the occupancy level started increasing from 07:00 and reached its peak of 5.3 at around 16:00, while the indoor CO_2 mixing ratio started increasing from about 420 ppm at 07:00 and peaked at about 600 ppm at 15:30. As expected, human exhaled breath is the major source of CO_2 in this office environment. However, monitoring indoor CO_2 remains critical in environments where other CO_2 sources exist, such as in indoor swimming pool facilities (e.g. CO_2 addition for maintaining water pH balance) and cooking with combustion sources (e.g. gas stoves).

The automated multi-point sampling system enables further examination of the spatial distribution of O_3 and CO_2 mixing ratios throughout the HVAC system. The O_3 mixing ratios along the supply air duct (sampled at Pre-Filter, Post-Filter, After HF, and SMSA) were relatively consistent, whereas the difference between SMSA and SMRA is markedly greater. This indicates that the contribution of the HVAC filter bank and supply air duct surfaces to the loss of O_3 is less than that for the office space itself (see discussion in Section 3.3). The spatial distribution of O_3 and CO_2 at OA, RA (SMRA and PHRA), and SMSA are strongly connected with the HVAC system operational mode. Comparing indoor O_3 and CO_2 mixing ratios under the three ventilation modes, mode 3 with the highest outdoor AER resulted in the highest SMRA O_3 mixing ratio and the lowest SMRA CO_2 mixing ratio. At low outdoor AERs (Fig. 3(a.) and 3(b.)), indoor O_3 and CO_2 mixing ratios peaked at approximately 14 ppb and 610 ppm, respectively. When outdoor AERs were raised to medium (Fig. 3(c.) and 3(d.)) and high levels (Fig. 3(e.) and 3(f.)), the peak indoor O_3 mixing ratios increased to about 25 and 34 ppb, while the peak indoor CO_2 mixing ratios dropped to around 510 and 490 ppm, respectively.

Similarly, under the three pressurized ventilation operational modes 4 to 6, spatiotemporal trends were observed across the seven sampling locations (CA not shown) throughout the HVAC system (Fig. 4). The SMRA O_3 mixing ratios peaked at 16, 29, and 41 ppb under ventilation modes 4 to 6 with low, medium, and high outdoor AERs, respectively. The indoor O_3 mixing ratios under the pressurized ventilation modes were generally higher than those under the non-pressurized ventilation modes mainly due to the bias of the sampling periods – the pressurized ventilation modes were implemented in May and June 2019, during which the outdoor O_3 mixing ratios were also higher. With lower outdoor O_3 mixing ratios, the modeled indoor O_3 ratios under the

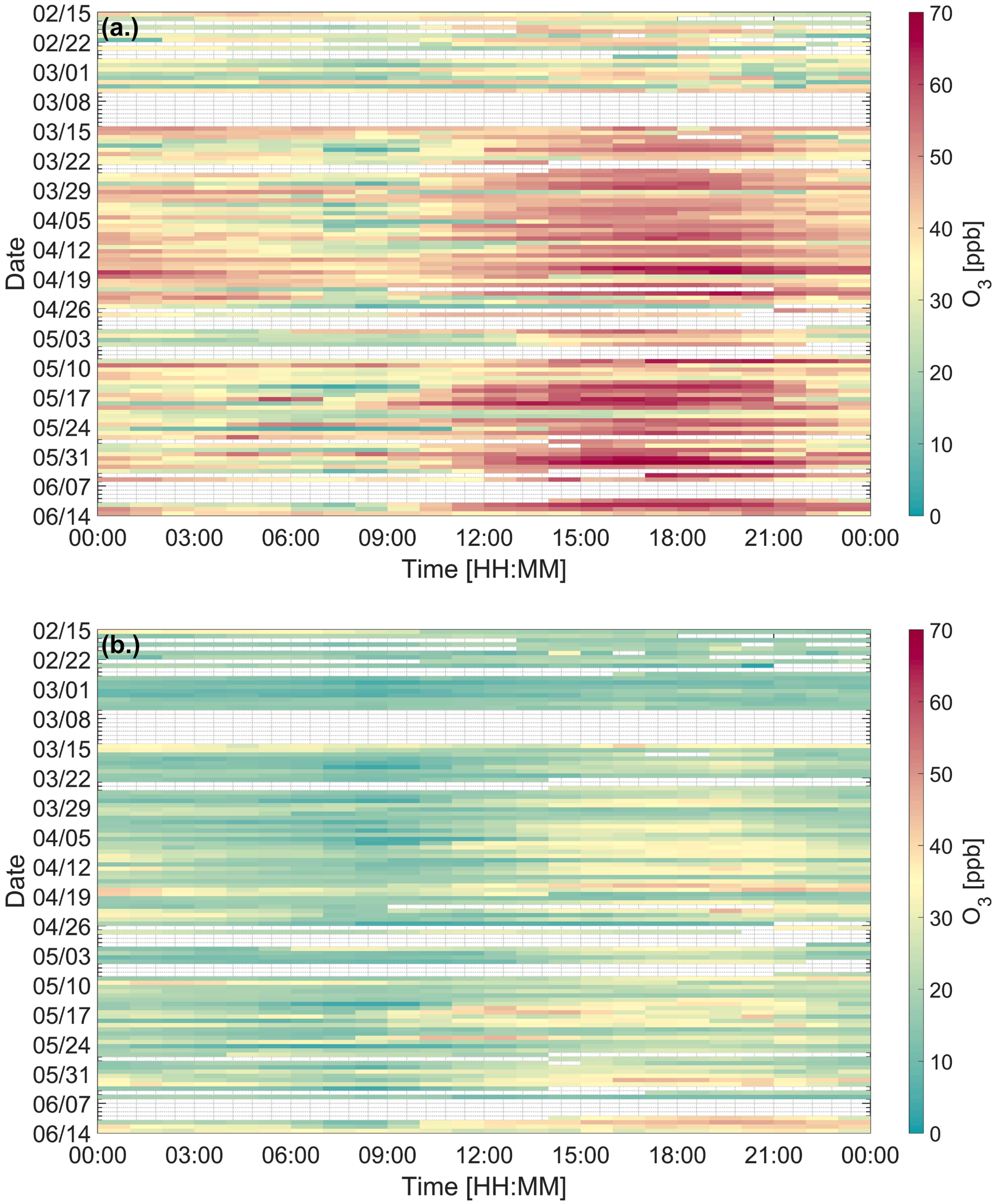

Fig. 5. Seasonal variation of (a.) outdoor O_3 mixing ratios and (b.) indoor O_3 mixing ratios. The blank areas indicate when measurement data was not available.

pressurized ventilation modes dropped as compared to their original levels (Fig. S1). Comparing mode 1 and mode 4 – low outdoor AER without and with pressurization – the outdoor O_3 mixing ratios under mode 4 were about 1.5 to 2 times higher than the outdoor O_3 mixing ratios under mode 1, while the indoor O_3 mixing ratios under the two modes were around the same levels. This indicates that pressurizing the room can effectively prevent outdoor air pollutants from infiltrating into indoor environments.

Fig. 5 shows the diurnal and seasonal variations of indoor and outdoor O_3 mixing ratios during the measurement campaign. The ranges for diurnal outdoor O_3 mixing ratios increased from 10 to 30 ppb in February/March to 20 to 60 ppb in June with the increase in the duration of daylight. The trend observed in this study agrees with the seasonal O_3 variations observed in the Midwest region of the U.S. [57]. The median indoor O_3 mixing ratios during the campaign varied from 15 to 25 ppb throughout the day, while the median outdoor O_3 mixing ratios varied from 15 to 60 ppb (Fig. 6). This suggests that the building operation strategy for maintaining acceptable IAQ cannot be simply based on CO_2 mixing ratios. For instance, when the occupancy level is high, the typical control strategy is to increase the outdoor AER.

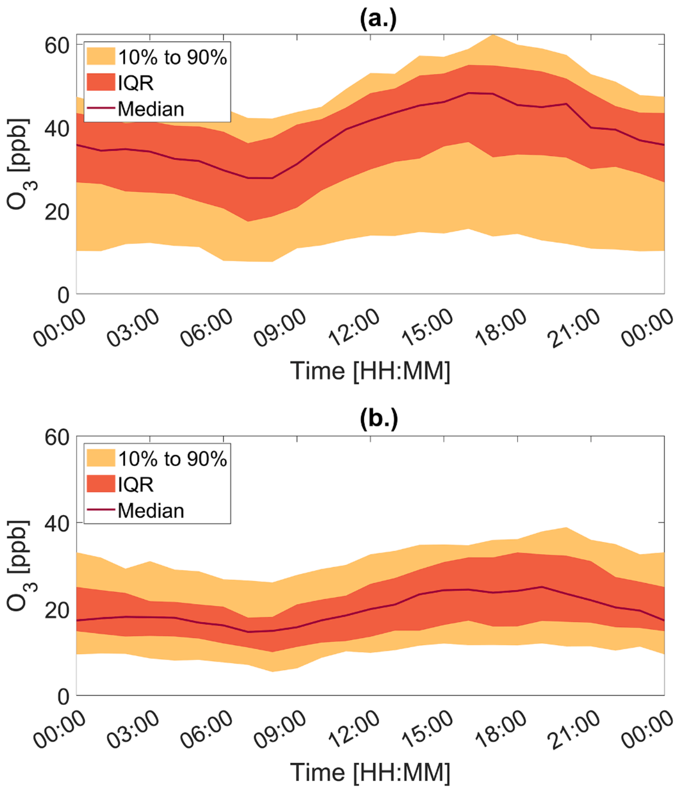

Fig. 6. Median, interquartile range, and 10th- to 90th-percentile of (a.) outdoor O_3 mixing ratios and (b.) indoor O_3 mixing ratios.

However, introducing more outdoor air to dilute indoor-generated CO_2 in the summer can lead to significant increases in indoor O_3 mixing ratios due to the high outdoor O_3 mixing ratios. With high occupancy levels and elevated O_3 mixing ratios, it is more likely that O_3 reactions with human skin lipids and body surfaces would form more secondary products that may potentially lead to adverse health effects. Thus, it is critical to consider the combined effects of different trace gases on IAQ when controlling a building ventilation system.

3.2. *O_3 and CO_2 I/O ratios under different outdoor AERs and human occupancy levels*

Spatiotemporal sampling of O_3 and CO_2 under different HVAC system operational modes revealed relationships between human occupancy, outdoors AERs, and O_3 and CO_2 mixing ratios. Given that outdoor O_3 is the major source of indoor O_3 in the office environment, the dependence of indoor O_3 mixing ratios on the outdoor AER and occupancy could be biased by the outdoor O_3 concentration. The indoor/outdoor (I/O) ratio normalizes indoor mixing ratios by outdoor mixing ratios, providing a more unbiased term to examine the contribution of indoor- and outdoor-associated sources of trace gases. Fig. 7 groups the I/O ratios of O_3 and CO_2 mixing ratios by outdoor AERs and office occupancy levels. The occupancy levels were categorized as: (1.) low occupancy where occupancy $<$ 4; (2.) medium occupancy where 4 $\leq$ occupancy $<$ 8; and (3.) high occupancy where occupancy $\geq$ 8.

Generally, the I/O ratio of O_3 increases with an increase in the outdoor AER (Fig. 7(a.)). Median O_3 I/O ratios ranged from 0.35 to 0.43, 0.45 to 0.55, and 0.60 to 0.65 at low, medium, and high AERs, respectively. O_3 I/O ratios observed in this study are consistent with the I/O ratio reported for an office in the U.S. with similar AERs [60], but higher than those reported in offices in Europe and Asia where AERs were not specified [61,62]. The dependency of the O_3 I/O ratio on occupancy levels varies with outdoor AERs. The median O_3 I/O ratio decreased by 11 to 22% from low/medium occupancy to high occupancy levels at low outdoor AERs, and by 4 to 22% at medium outdoor AERs. Interestingly, at high outdoor AERs, the median O_3 I/O ratios were around the same level as at low and medium occupancy, and only elevated by 8% from low/medium to high occupancy levels. At lower AERs, air exchange due to ventilation contributed less to the loss mechanisms of indoor O_3, while O_3 deposition to human body surfaces contributed more to the loss of indoor O_3. Thus, with higher occupancy, lower I/O ratios can be observed, as the increase of O_3 deposition leads to lower indoor O_3 mixing ratios. In contrast, at higher AERs, outdoor air ventilation via the HVAC system became the major sink for indoor O_3 and deposition to occupant surfaces contributed less to indoor O_3 loss, so the O_3 I/O ratio can be less dependent on occupancy levels at higher AERs. An ANOVA analysis (Table 4) also verified the dependence of the O_3 I/O ratio on occupancy and AER ($p < 0.001$).

Fig. 7(b.) presents the "O_3 loss" at different AERs and occupancy levels. The median value of the O_3 loss at different outdoor AERs and occupancy levels varies from 14.7 to 26.5 ppb, similar to the O_3 loss ranges modeled by Weschler and Nazaroff (15.5 to 27.8 ppb) for different indoor environments with AERs from 0.25 to 6 h^{-1} and occupancy levels from 2 to 35 occupants [56]. At low and medium AERs, the O_3 loss increased with the increase in occupancy levels due to deposition onto human body surfaces. This indicates more secondary products can be formed indoors with higher occupancy, which may lead to adverse health effects. The O_3 loss decreased when the outdoor AER increased, as higher AER leads to elevated indoor O_3 mixing ratios. This suggests that HVAC system control and building ventilation strategies need to be adjusted accordingly based on the outdoor AER and occupancy levels.

Fig. 7(c.) illustrates the dependency of the CO_2 I/O ratio on the AER and occupancy levels. Occupants are the major source of indoor CO_2 and the median CO_2 I/O ratios increased with the increase of occupancy levels, increasing from 1.01 to 1.03 (low occupancy) to 1.22 to 1.45 (high occupancy) at various AERs. However, the increase in the outdoor AER did not always lower the CO_2 I/O ratio. At low and medium occupancy (less than 8 occupants), the median CO_2 I/O ratios were similar across low, medium, and high AERs. The consistency in CO_2 I/O ratios across different AERs indicates that with lower occupancy, a low AER would be sufficient to control the indoor CO_2 mixing ratio at low levels, with an I/O ratio very close to 1. At high occupancy levels ($>$ 8 occupants), the CO_2 I/O ratio dropped by 5% and 15% when the AER increased from low to medium and high levels, respectively. Increasing outdoor AERs can effectively dilute indoor-generated CO_2 at higher occupancy levels. Fig. 7 demonstrates that the outdoor AERs and occupancy levels may have different effects on O_3 and CO_2 I/O ratios. Building ventilation strategies may need to be implemented with careful and comprehensive consideration of their impact on different indoor air pollutants. Recent studies have evaluated the performance of low-cost metal oxide and electrochemical sensors for trace gases, including O_3, CO, and NO_x [63–65]. With proper calibration, these low-cost sensors showed good correlation with reference analytical instruments. A multi-point trace gas sampling system such as that presented in this study, or implemented through the use of low-cost sensor arrays, has the potential to be integrated into building automation systems to aid the ventilation control of buildings and improve IAQ.

3.3. *O_3 loss in the office and its HVAC system*

Fig. 8 illustrates diurnal trends of overall and itemized O_3 loss rates during representative days for three different ventilation operational modes – 1, 2, and 3. The loss rate due to O_3 deposition to human body surfaces generally follows the trend of indoor occupancy levels, indicating that the occupancy level is strongly connected to indoor O_3 loss mechanisms and indoor O_3 mixing ratios. For the ventilation mode 1 with the lowest AER, the overall O_3 loss rate ranges from 5.3 to 9.2 h^{-1} throughout the day. This variation is mainly due to the variation in O_3 deposition to human body surfaces, which ranges from 0 to 2.3 h^{-1} with occupancy ranging from 0 to 9.5. O_3 loss due to ventilation and

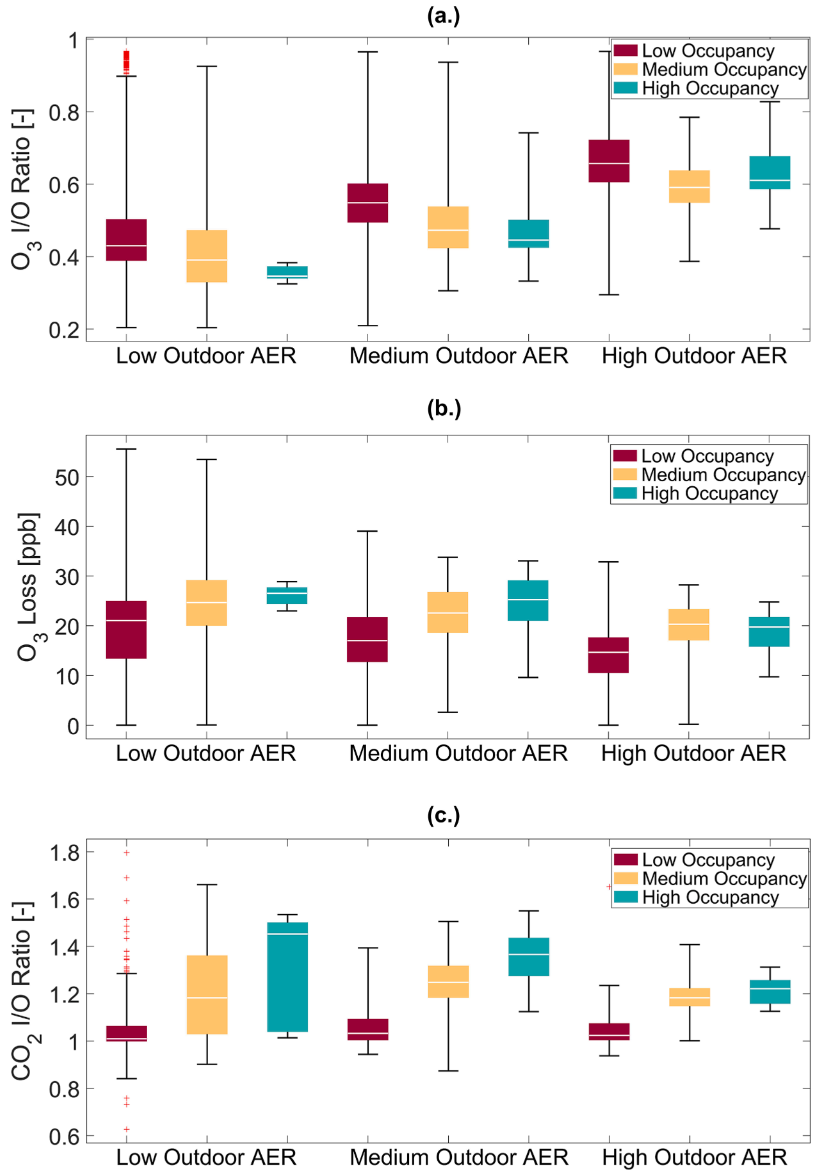

Fig. 7. (a.) I/O ratios of O_3 mixing ratios, (b.) O_3 loss, and (c.) I/O ratios of CO_2 mixing ratios for different outdoor AERs and office occupancy levels during the field measurement campaign.

Table 4
ANOVA test for the dependence of the O_3 I/O ratio on AER and occupancy.

	Sum of Squares	DF	Sum of Squares	F	p-Value
AER	19.007	3	6.3357	394.82	1.46E-226
Occupancy	2.5740	2	1.2870	80.203	6.33E-35
Error	69.114	4307	0.016047		
Total	90.296	4312			

exfiltration dominated the overall O_3 loss rate under all three ventilation modes for our study site, an office environment without indoor combustion sources (e.g. gas stoves). Outdoor air ventilation and exfiltration, deposition to building material surfaces, and deposition to human body surfaces account for 37 to 64%, 36 to 37%, and 0 to 26% of the overall O_3 loss rate, respectively. The contribution of gas-phase reactions to the overall O_3 loss rate was negligible. It should be noted that in other indoor environments, especially those with combustion sources and the use of personal care products, O_3 reactions with NO_x and VOCs could be important sinks. The overall O_3 loss rates were the highest, approaching a peak of around 14 h^{-1}, under ventilation mode 3 with the highest outdoor AER. Outdoor air ventilation contributed 44 to 51% to the overall O_3 loss rate under mode 2 and 56 to 69% to the overall O_3 loss rate under mode 3. For O_3 deposition to human body surfaces, the loss rate peaked at 3.0 h^{-1} and 2.6 h^{-1} when the office occupancy level peaked at 8.7 and 5.5 under ventilation modes 2 and 3, respectively. Average O_3 deposition velocities to human body surfaces during the three days selected from ventilation modes 1 to 3 were estimated to be 48, 68, and 93 m h^{-1}, which results in O_3 loss rates of 0.25, 0.35, and 0.47 h^{-1} $person^{-1}$, respectively. The deposition velocities to human body surfaces observed in this study were 2 to 10 times higher than the values reported in previous studies [12,16,66–68]. O_3 loss rates reported in these studies vary from 0.02 h^{-1} $person^{-1}$ to 1.5 h^{-1} $person^{-1}$, with room volumes ranging from 22.5 to 670 m^3. O_3 loss rates observed in our study were 1.5 to 4.7 times higher than the O_3 loss rates for a simulated office with a similar room volume [69]. Such inconsistencies might be explained by differences in the application of personal care products to the skin and hair [70] or the clothing the occupants were wearing [13, 71], especially for mode 3 which occurred in late April. The deposition velocities can be enhanced due to O_3 reactions with hair (large surface

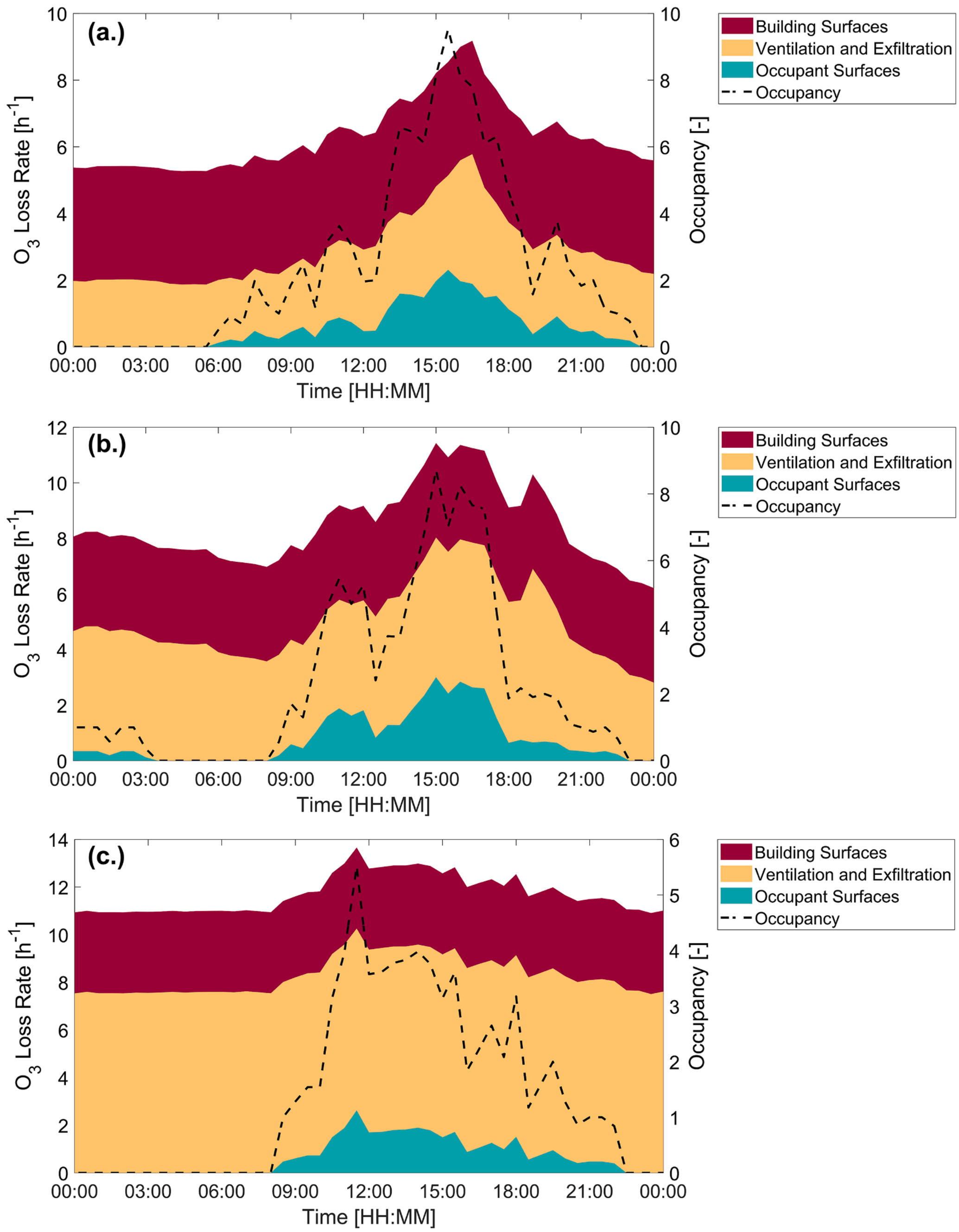

Fig. 8. Diurnal trends of the overall and itemized O_3 loss rates (left axis) and occupancy (right axis) during representative days for three different ventilation modes: (a.) ventilation mode 1, (b.) ventilation mode 2, and (c.) ventilation mode 3.

area), soiled clothing (multiple layers may be worn), and soiled backpacks. Thus, the assumed occupant surface area might be underestimated. Time delays in indoor and outdoor O_3 sampling and the time-averaged loss rate calculation may also lead to uncertainties in the estimation of the deposition velocities.

Considering the large surface area of the HVAC system and its components, the HVAC system can be another important sink of outdoor O_3 being supplied to indoor environments. The multi-point sampling system allows for the investigation of how each HVAC component can impact O_3 dynamics. Fig. 9(a.) presents the diurnal trend of O_3 loss across the HVAC filter bank during the pre/post-filter sequence. Pre-Filter O_3 mixing ratios were consistently higher than the Post-Filter mixing ratios, indicating O_3 deposition to the filter media. Up to 8 ppb of O_3 could deposit to the HVAC filter bank when passing through, resulting in 0 to 10% of O_3 loss across the filter. O_3 removal by other HVAC system components is presented in Fig. 9(b.). O_3 mixing ratios dropped by a median of 3.9, 1.2, 0.5, and 6.0% when travelling from Pre-Filter to SMSA, Post-Filter to SMSA, After HF to SMSA, and SMRA to PHRA, respectively. The difference between O_3 removal percentages from Pre-Filter and Post-Filter to SMSA verifies the contribution of the HVAC filter bank to O_3 deposition. For the other parts of the HVAC system, the HVAC duct itself could be major contributor of O_3 loss. The HVAC duct between SMRA and PHRA was the longest among the four segments, with only one return fan installed along the duct. Both sampling locations were located along the return air duct, however, up to 18% of O_3 loss was observed. With the two sampling locations at two different mechanical rooms that are > 10 m apart, the large surface area of the long HVAC duct contributes to the high O_3 loss from SMRA to

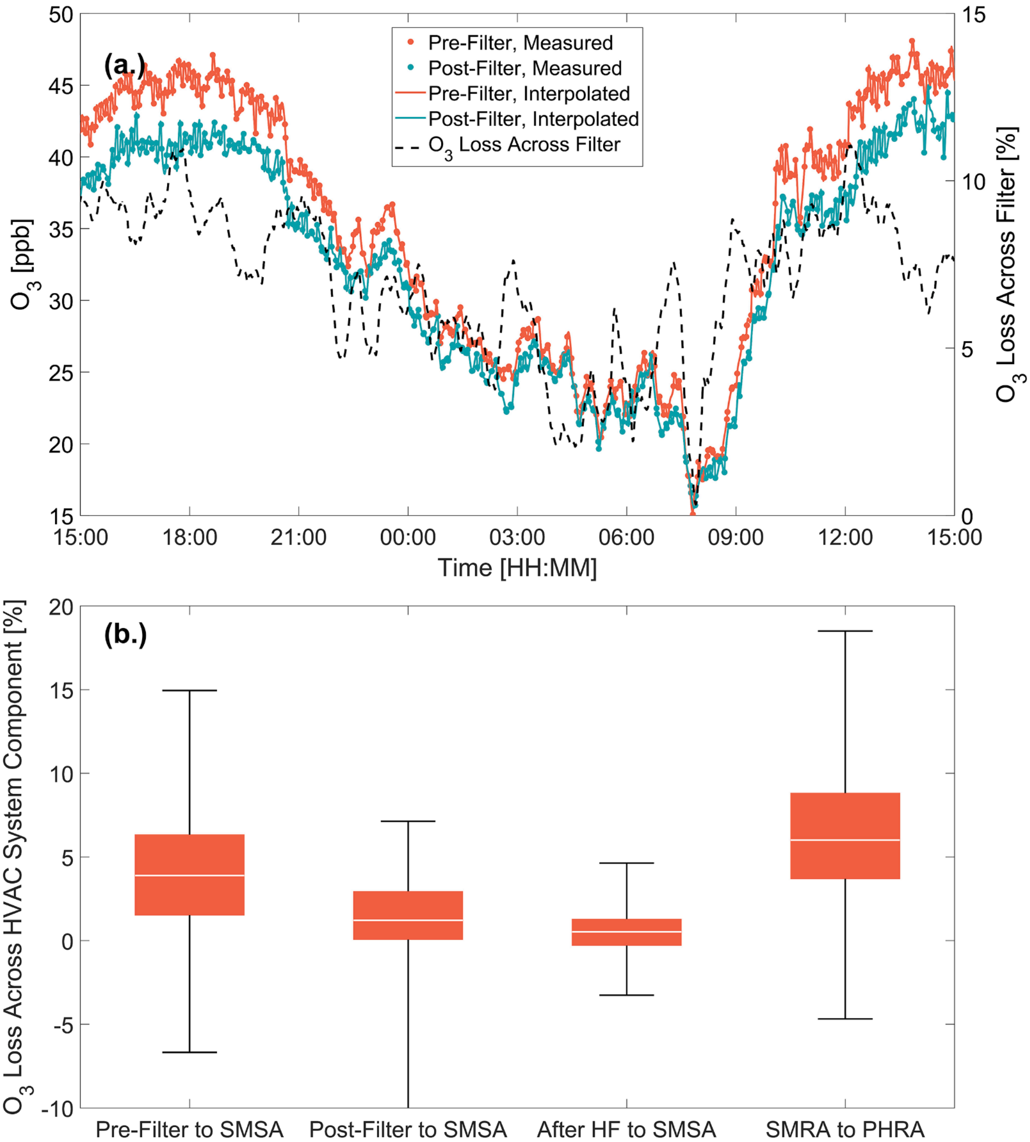

Fig. 9. (a.) Diurnal trend of the O_3 loss across the HVAC filter bank during the pre-/post-filter sampling sequence and (b.) O_3 loss across different HVAC system components during the field measurement campaign.

PHRA.

It is important to note that the findings presented here may be specific to the office environment studied. In office settings, as demonstrated in this study, occupants are major contributors to O_3 loss, with large-scale and complex HVAC systems also playing an important role in the removal of O_3. In contrast, in residential environments with lower occupancy and simpler HVAC systems, the contribution of occupants and HVAC systems to O_3 loss may be less significant. However, other indoor activities – such as cooking with gas stoves, which emit NO_x, or the use of personal care products that release VOCs – can lead to O_3 reactions with these compounds and the production of secondary pollutants. These processes may become the dominant mechanisms for O_3 loss in such environments. This highlights the need for multi-point sampling of trace gases across diverse indoor environments and their associated HVAC systems to fully understand the fate and dynamics of indoor air pollutants.

4. Conclusions and future directions

This study introduced a novel automated multi-point sampling system for the real-time monitoring of spatiotemporal trends of trace gases in the HVAC system of a LEED-certified office building. A four-month field measurement campaign at the Purdue University Ray W. Herrick Laboratories provided valuable insights into the dynamics of O_3 and CO_2 within the HVAC system under varying ventilation modes and occupancy levels. Through O_3 and CO_2 measurements with the multi-point sampling system at eight different locations throughout the HVAC system in a LEED-certified office building, spatiotemporal variations in O_3 and CO_2 mixing ratios were observed. The results revealed significant diurnal and seasonal variations in both indoor and outdoor O_3 mixing ratios, emphasizing the influence of outdoor air on IAQ. Higher outdoor AERs were associated with increased indoor O_3 levels but reduced CO_2 concentrations, demonstrating the complex interplay between ventilation rates and indoor air pollutant levels. Spatial variations of O_3 and CO_2 mixing ratios were observed as well, especially across supply air, return air, and outdoor air sampling locations. Minor variations were also observed among different locations along the supply duct (Pre-Filter, Post-Filter, After-HF, and SMSA) and return duct (SMRA and PHRA), indicating that the HVAC filter bank and duct surfaces can contribute to O_3 loss.

I/O ratios of O_3 and CO_2 ranged from 0.35 to 0.65 and 1.01 to 1.45, respectively, at different outdoor AERs and occupancy levels.

Ventilation and occupancy impact the I/O ratio of O_3 and CO_2 differently, which needs to be carefully accounted for when implementing building ventilation strategies to improve IAQ. Overall O_3 loss rates and the contribution of each loss mechanism were estimated, including building ventilation and exfiltration (outdoor air exchange), gas-phase O_3 reactions with NO_x and selected VOCs, and O_3 deposition to building material surfaces and human body surfaces. Ventilation and exfiltration contributed most to the overall O_3 loss rate, and the contribution of deposition on human body surfaces cannot be neglected when the occupancy level is high. Human occupancy significantly influenced O_3 deposition onto skin and clothing, further complicating the dynamics of IAQ. This study also highlighted the role of HVAC components, such as filters and ducts, in contributing to O_3 loss, with up to 18% O_3 removal observed in the longest HVAC duct segment.

Current ventilation standards, which primarily consider CO_2 mixing ratios in the design of the ventilation rate, may not adequately address the complexities of indoor air composition and the interactions between various pollutants. This study emphasizes the need for a more comprehensive IAQ sensing system and ventilation control strategies that consider multiple trace gases to effectively optimize IAQ. The automated multi-point sampling system presented in this study has the potential to be implemented in building automation systems to aid in the control of building ventilation. This system can be connected not only to CO_2 and O_3 analyzers as demonstrated in this study, but also to advanced analytical instruments, including online mass spectrometers such as PTR-TOF-MS, which can characterize a wide range of VOCs. While installing individual instruments at each sampling location would be impractical due to their size, cost, and calibration needs, a multi-point sampling system with an automatic multi-port valve offers a practical solution for precise spatiotemporal trace gas monitoring. By integrating this system into building automation systems, real-time data of multiple trace gases (e.g. CO_2, O_3, NO_x, VOCs) can be utilized to develop dynamic ventilation strategies that respond to varying indoor and outdoor conditions. For example, by measuring trace gases at the supply, return, and outdoor air ducts, building automation systems can better understand the sources, transport, and fate of these air pollutants.

Real-time monitoring of the spatial distribution of trace gases at these locations can be further inputted into indoor chemistry models to predict the concentration of these pollutants and their possible secondary reaction products in order to find optimal settings for the HVAC system. This dynamic approach helps maintain a healthy indoor environment while minimizing energy consumption by avoiding unnecessary ventilation during periods of high outdoor air pollution. In addition, by arranging the sampling locations upstream and downstream of in-duct air filtration and purification devices (such as HVAC filter banks, UV disinfection units, or bi-polar ionization devices), the system can evaluate the in-situ performance of these technologies, ensuring that these devices are functioning properly and informing when maintenance is needed. We believe that the innovative integration of automated multi-point sampling, analytical instrumentation, and building automation systems opens up new possibilities for real-time air quality monitoring and predicting and enabling more accurate and efficient HVAC system operation and maintenance across diverse indoor environments. Such systems have the potential to help reduce building maintenance and operational costs while improving the health and productivity of office workers. Future research should focus on exploring their integration with other smart building technologies, optimizing the control of HVAC systems, analyzing their cost benefits, and evaluating their long-term benefits in diverse building types and climates.

CRediT authorship contribution statement

Jinglin Jiang: Writing – review & editing, Writing – original draft, Visualization, Validation, Methodology, Investigation, Formal analysis, Data curation. **Junkai Huang:** Visualization, Methodology, Formal analysis. **Nusrat Jung:** Writing – review & editing, Writing – original draft, Visualization, Validation, Supervision, Software, Resources, Project administration, Methodology, Investigation, Funding acquisition, Formal analysis, Data curation, Conceptualization. **Brandon E. Boor:** Writing – review & editing, Writing – original draft, Visualization, Validation, Supervision, Software, Resources, Project administration, Methodology, Investigation, Funding acquisition, Formal analysis, Data curation, Conceptualization.

Declaration of competing interest

The authors declare that they have no conflict of interest.

Acknowledgements

Financial support was provided by the National Science Foundation (CBET-1847493 to B.E.B.), Purdue University start-up funds (to N.J.), a Purdue University Bilsland Dissertation Fellowship (to J.J.), and an American Society of Heating, Refrigerating, and Air Conditioning Engineers Graduate Student Grant-In-Aid Award (to J.J.). The authors would like to thank the staff at the Ray W. Herrick Laboratories for their support in conducting the air pollutant measurements in the Herrick Living Laboratory office.

Supplementary materials

Supplementary material associated with this article can be found, in the online version, at doi:10.1016/j.buildenv.2025.112651.

Data availability

Data will be made available on request.

References

[1] Y. Al horr, M. Arif, M. Katafygiotou, A. Mazroei, A. Kaushik, E. Elsarrag, Impact of indoor environmental quality on occupant well-being and comfort: a review of the literature, Int. J. Sustain. Built Environ. 5 (2016) 1–11, https://doi.org/10.1016/J.IJSBE.2016.03.006.
[2] H. Parhizkar, P. Taddei, D. Weziak-Bialowolska, E. McNeely, J.D. Spengler, J. G. Cedeño Laurent, Objective indoor air quality parameters and their association to respiratory health and well-being among office workers, Build. Environ. 246 (2023) 110984, https://doi.org/10.1016/J.BUILDENV.2023.110984.
[3] Z. Pei, B. Lin, Y. Liu, Y. Zhu, Comparative study on the indoor environment quality of green office buildings in China with a long-term field measurement and investigation, Build. Environ. 84 (2015) 80–88, https://doi.org/10.1016/J.BUILDENV.2014.10.015.
[4] K. Azuma, N. Kagi, U. Yanagi, H. Osawa, Effects of low-level inhalation exposure to carbon dioxide in indoor environments: a short review on human health and psychomotor performance, Environ. Int. 121 (2018) 51–56, https://doi.org/10.1016/J.ENVINT.2018.08.059.
[5] W.M. Alberts, Indoor air pollution: NO, NO_2, CO, and CO_2, J. Allergy Clin. Immunol. 94 (1994) 289–295, https://doi.org/10.1053/AI.1994.V94.A56007.
[6] J. Jiang, X. Ding, A. Tasoglou, H. Huber, A.D. Shah, N. Jung, B.E. Boor, Real-time measurements of botanical disinfectant emissions, transformations, and multiphase inhalation exposures in buildings, Environ. Sci. Technol. Lett. 8 (2021) 558–566, https://doi.org/10.1021/ACS.ESTLETT.1C00390.
[7] C.M.F. Rosales, J. Jiang, A. Lahib, B.P. Bottorff, E.K. Reidy, V. Kumar, A. Tasoglou, H. Huber, S. Dusanter, A. Tomas, B.E. Boor, P.S. Stevens, Chemistry and human exposure implications of secondary organic aerosol production from indoor terpene ozonolysis, Sci. Adv. 8 (2022) eabj9156, https://doi.org/10.1126/sciadv.abj9156.
[8] A.W. Nørgaard, J.D. Kudal, V. Kofoed-Sørensen, I.K. Koponen, P. Wolkoff, Ozone-initiated VOC and particle emissions from a cleaning agent and an air freshener: risk assessment of acute airway effects, Environ. Int. 68 (2014) 209–218, https://doi.org/10.1016/j.envint.2014.03.029.
[9] T. Wainman, J. Zhang, C.J. Weschler, P.J. Lioy, Ozone and limonene in indoor air: a source of submicron particle exposure, Environ. Health Perspect. 108 (2000) 1139–1145, https://doi.org/10.1289/ehp.001081139.
[10] S. Youssefi, M.S. Waring, Transient secondary organic aerosol formation from D-limonene and a-pinene ozonolysis in indoor environments, Environ. Sci. Technol. (2014) 145–152, https://doi.org/10.1021/es5009906.
[11] E. Vartiainen, M. Kulmala, T.M. Ruuskanen, R. Taipale, J. Rinne, H. Vehkamäki, Formation and growth of indoor air aerosol particles as a result of D-limonene oxidation, Atmos. Environ. 40 (2006) 7882–7892, https://doi.org/10.1016/j.atmosenv.2006.07.022.

[12] C.J. Weschler, W.W. Nazaroff, Human skin oil: a major ozone reactant indoors, Environ. Sci. Atmos. 3 (2023) 640–661, https://doi.org/10.1039/D3EA00008G.

[13] P.S.J. Lakey, G.C. Morrison, Y. Won, K.M. Parry, M. von Domaros, D.J. Tobias, D. Rim, M. Shiraiwa, The impact of clothing on ozone and squalene ozonolysis products in indoor environments, Commun. Chem. 2 (2019) 1–8, https://doi.org/10.1038/s42004-019-0159-7.

[14] C. Wang, M.S. Waring, Secondary organic aerosol formation initiated from reactions between ozone and surface-sorbed squalene, Atmos. Environ. 84 (2014) 222–229, https://doi.org/10.1016/J.ATMOSENV.2013.11.009.

[15] S. Zhou, M.W. Forbes, J.P.D. Abbatt, Kinetics and products from heterogeneous oxidation of squalene with ozone, Environ. Sci. Technol. 50 (2016) 11688–11697, https://doi.org/10.1021/acs.est.6b03270.

[16] A. Wisthaler, C.J. Weschler, Reactions of ozone with human skin lipids: sources of carbonyls, dicarbonyls, and hydroxycarbonyls in indoor air, Proc. Natl. Acad. Sci. U. S. A. 107 (2010) 6568–6575, https://doi.org/10.1073/pnas.0904498106.

[17] U.S. EPA, Integrated Science Assessment for Ozone and Related Photochemical Oxidants (Final). (2024).

[18] K. Zu, X. Liu, L. Shi, G. Tao, C.T. Loftus, S. Lange, J.E. Goodman, Concentration-response of short-term ozone exposure and hospital admissions for asthma in Texas, Environ. Int. 104 (2017) 139–145, https://doi.org/10.1016/J.ENVINT.2017.04.006.

[19] A. Zanobetti, J. Schwartz, Mortality displacement in the association of ozone with mortality an analysis of 48 cities in the United States, Am. J. Respir. Crit. Care Med. 177 (2024) 184–189. 10.1164/rccm.200706-823OC.

[20] C. Yang, H. Yang, S. Guo, Z. Wang, X. Xu, X. Duan, H. Kan, Alternative ozone metrics and daily mortality in Suzhou: the China Air Pollution and Health Effects Study (CAPES), Sci. Total Environ. 426 (2012) 83–89. 10.1016/j.scitotenv.2012.03.036.

[21] M.C. Turner, M. Jerrett, C.A. Pope, D. Krewski, S.M. Gapstur, W.R. Diver, B. S. Beckerman, J.D. Marshall, J. Su, D.L. Crouse, R.T. Burnett, Long-term ozone exposure and mortality in a large prospective study, Am. J. Respir. Crit. Care Med. 193 (2016) 1134–1142, https://doi.org/10.1164/RCCM.201508-1633OC.

[22] S.E. Anderson, J.R. Wells, A. Fedorowicz, L.F. Butterworth, B.J. Meade, A. E. Munson, Evaluation of the contact and respiratory sensitization potential of volatile organic compounds generated by simulated indoor air chemistry, Toxicol. Sci. 97 (2007) 355–363, https://doi.org/10.1093/TOXSCI/KFM043.

[23] S.E. Anderson, J. Franko, L.G. Jackson, J.R. Wells, J.E. Ham, B.J. Meade, Irritancy and allergic responses induced by exposure to the indoor air chemical 4-oxopentanal, Toxicol. Sci. 127 (2012) 371–381, https://doi.org/10.1093/TOXSCI/KFS102.

[24] J. Jarvis, M.J. Seed, R.A. Elton, L. Sawyer, R.M. Agius, Relationship between chemical structure and the occupational asthma hazard of low molecular weight organic compounds, Occup. Environ. Med. 62 (2005) 243–250, https://doi.org/10.1136/OEM.2004.016402.

[25] S.E. Anderson, L.G. Jackson, J. Franko, J.R. Wells, Evaluation of dicarbonyls generated in a simulated indoor air environment using an in vitro exposure system, Toxicol. Sci. 115 (2010) 453–461, https://doi.org/10.1093/TOXSCI/KFQ067.

[26] Y. Lu, J. Huang, D.N. Wagner, Z. Lin, N. Jung, B.E. Boor, The influence of displacement ventilation on indoor carbon dioxide exposure and ventilation efficiency in a living laboratory open-plan office, Build. Environ. 256 (2024) 111468, https://doi.org/10.1016/J.BUILDENV.2024.111468.

[27] Á. Muelas, P. Remacha, A. Pina, E. Tizné, S. El-Kadmiri, A. Ruiz, D. Aranda, J. Ballester, Analysis of different ventilation strategies and CO_2 distribution in a naturally ventilated classroom, Atmos. Environ. 283 (2022) 119176, https://doi.org/10.1016/J.ATMOSENV.2022.119176.

[28] J.F. Belmonte, R. Barbosa, M.G. Almeida, CO_2 concentrations in a multifamily building in Porto, Portugal: occupants' exposure and differential performance of mechanical ventilation control strategies, J. Build. Eng. 23 (2019) 114–126, https://doi.org/10.1016/J.JOBE.2019.01.008.

[29] O.A. Seppänen, W.J. Fisk, M.J. Mendell, Association of ventilation rates and CO_2 concentrations with health andother responses in commercial and institutional buildings, Indoor Air 9 (1999) 226–252, https://doi.org/10.1111/J.1600-0668.1999.00003.X.

[30] D. Zhang, P.M. Bluyssen, Exploring the possibility of using CO_2 as a proxy for exhaled particles to predict the risk of indoor exposure to pathogens, Indoor Built Environ. 32 (2023) 1958–1972, https://doi.org/10.1177/1420326X221110043.

[31] O. Ramalho, G. Wyart, C. Mandin, P. Blondeau, P.A. Cabanes, N. Leclerc, J. U. Mullot, G. Boulanger, M. Redaelli, Association of carbon dioxide with indoor air pollutants and exceedance of health guideline values, Build. Environ. 93 (2015) 115–124, https://doi.org/10.1016/J.BUILDENV.2015.03.018.

[32] L. Chatzidiakou, D. Mumovic, A. Summerfield, Is CO_2 a good proxy for indoor air quality in classrooms? Part 1: the interrelationships between thermal conditions, CO_2 levels, ventilation rates and selected indoor pollutants, Build. Serv. Eng. Res. Technol. 36 (2015) 129–161, https://doi.org/10.1177/0143624414566244.

[33] ASHRAE, ANSI/ASHRAE Standard 62.1-2022 Ventilation and Acceptable Indoor Air Quality, 2022.

[34] C.J. Weschler, Ozone's impact on public health: contributions from indoor exposures to ozone and products of ozone-initiated chemistry, Environ. Health Perspect. 114 (2006) 1489–1496, https://doi.org/10.1289/ehp.9256.

[35] C.J. Weschler, Ozone in indoor environments: concentration and chemistry, Indoor Air 10 (2000) 269–288, https://doi.org/10.1034/J.1600-0668.2000.010004269.X.

[36] W.W. Nazaroff, C.J. Weschler, Indoor ozone: concentrations and influencing factors, Indoor Air 32 (2022), https://doi.org/10.1111/INA.12942.

[37] G.C. Morrison, W.W. Nazaroff, J. Alejandro Cano-Ruiz, A.T. Hodgson, M. P. Modera, Indoor air quality impacts of ventilation ducts: ozone removal and emissions of volatile organic compounds, J. Air Waste Manag. Assoc. 48 (1998) 941–952, https://doi.org/10.1080/10473289.1998.10463740.

[38] M. Hyttinen, P. Pasanen, P. Kalliokoski, Removal of ozone on clean, dusty and sooty supply air filters, Atmos. Environ. 40 (2006) 315–325, https://doi.org/10.1016/J.ATMOSENV.2005.09.040.

[39] P. Zhao, J.A. Siegel, R.L. Corsi, Ozone removal by HVAC filters, Atmos. Environ. 41 (2007) 3151–3160, https://doi.org/10.1016/J.ATMOSENV.2006.06.059.

[40] D.W. Bearg, Indoor air quality and HVAC systems, Lewis Publishers, 1993.

[41] N. Nassif, A robust CO2-based demand-controlled ventilation control strategy for multi-zone HVAC systems, Energy Build. 45 (2012) 72–81, https://doi.org/10.1016/J.ENBUILD.2011.10.018.

[42] J. Li, J. Wall, G. Platt, Indoor air quality control of HVAC system, in: Proceedings of the 2010 International Conference on Modelling, Identification and Control, Okayama, Japan, 2010, pp. 756–761.

[43] G. Song, Z. Ai, Z. Liu, G. Zhang, A systematic literature review on smart and personalized ventilation using CO_2 concentration monitoring and control, Energy Rep. 8 (2022) 7523–7536, https://doi.org/10.1016/J.EGYR.2022.05.243.

[44] T. Wu, A. Tasoglou, H. Huber, P.S. Stevens, B.E. Boor, Influence of mechanical ventilation systems and human occupancy on time-resolved source rates of volatile skin oil ozonolysis products in a LEED-certified office building, Environ. Sci. Technol. 55 (2021) 16477–16488, https://doi.org/10.1021/acs.est.1c03112.

[45] T. Wu, A. Tasoglou, D.N. Wagner, J. Jiang, H.J. Huber, P.S. Stevens, N. Jung, B. E. Boor, Modern buildings act as a dynamic source and sink for urban air pollutants, Cell Rep. Sustain. 1 (2024) 100103, https://doi.org/10.1016/J.CRSUS.2024.100103.

[46] J. Jiang, X. Ding, K.P. Isaacson, A. Tasoglou, H. Huber, A.D. Shah, N. Jung, B. E. Boor, Ethanol-based disinfectant sprays drive rapid changes in the chemical composition of indoor air in residential buildings, J. Hazard. Mater. Lett. 2 (2021) 100042, https://doi.org/10.1016/J.HAZL.2021.100042.

[47] J. Liu, J. Jiang, X. Ding, S.S. Patra, J.N. Cross, C. Huang, V. Kumar, P. Price, E. K. Reidy, A. Tasoglou, H. Huber, P.S. Stevens, B.E. Boor, N. Jung, Real-time evaluation of terpene emissions and exposures during the use of scented wax products in residential buildings with PTR-TOF-MS, Build. Environ. 255 (2024) 111314, https://doi.org/10.1016/J.BUILDENV.2024.111314.

[48] X. Ding, H. Lu, J. Jiang, A. Tasoglou, A.D. Shah, N. Jung, Real-time indoor sensing of volatile organic compounds during building disinfection events via photoionization detection and proton transfer reaction mass spectrometry, Build. Environ. 246 (2023) 110953, https://doi.org/10.1016/J.BUILDENV.2023.110953.

[49] X. Ding, J. Jiang, A. Tasoglou, H. Huber, A.D. Shah, N. Jung, Evaluation of workplace exposures to volatile chemicals during COVID-19 building disinfection activities with proton transfer reaction mass spectrometry, Ann. Work Expo. Health (2023), https://doi.org/10.1093/ANNWEH/WXAC096.

[50] D.N. Wagner, A. Mathur, B.E. Boor, Spatial seated occupancy detection in offices with a chair-based temperature sensor array, Build. Environ. 187 (2021) 107360, https://doi.org/10.1016/J.BUILDENV.2020.107360.

[51] R. Atkinson, D. Hasegawa, S.M. Aschmann, Rate constants for the gas-phase reactions of O_3 with a series of monoterpenes and related compounds at 296 ± 2 K, Int. J. Chem. Kinet. 22 (1990) 871–887, https://doi.org/10.1002/KIN.550220807.

[52] R.A. Cox, M. Ammann, J.N. Crowley, H. Herrmann, M.E. Jenkin, V.F McNeill, A. Mellouki, J. Troe, T.J. Wallington, Evaluated kinetic and photochemical data for atmospheric chemistry: volume VII-Criegee intermediates, Atmos. Chem. Phys. 20 (2020) 13497–13519, https://doi.org/10.5194/ACP-20-13497-2020.

[53] R. Atkinson, D.L. Baulch, R.A. Cox, J.N. Crowley, R.F. Hampson, R.G. Hynes, M. E. Jenkin, M.J. Rossi, J. Troe, Evaluated kinetic and photochemical data for atmospheric chemistry: volume I-gas phase reactions of O_x, HO_x, NO_x and SO_x species, Atmos. Chem. Phys. 4 (2004) 1461–1738. https://acp.copernicus.org/articles/4/1461/2004//.

[54] NIST Chemical Kinetics Database, (2024). https://kinetics.nist.gov/kinetics/index.jsp (accessed June 29, 2024).

[55] D. Du Bois, E.F. Du Bois, A formula to estimate the approximate surface area if height and weight be known, Nutrition 5 (5) (1989) 303–311, discussion 312-3, https://api.semanticscholar.org/CorpusID:45693603.

[56] C.J. Weschler, W.W. Nazaroff, Ozone loss: a surrogate for the indoor concentration of ozone-derived products, Environ. Sci. Technol. 57 (2023) 13569–13578, https://doi.org/10.1021/acs.est.3c03968.

[57] E. Chan, R.J. Vet, Atmospheric chemistry and physics baseline levels and trends of ground level ozone in Canada and the United States, Atmos. Chem. Phys 10 (2010) 8629–8647, https://doi.org/10.5194/acp-10-8629-2010.

[58] B.K. Pun, C. Seigneur, W. White, Day-of-week behavior of atmospheric ozone in three U.S. cities, J. Air Waste Manag. Assoc. 53 (2003) 789–801, https://doi.org/10.1080/10473289.2003.10466231.

[59] J.M. Heuss, D.F. Kahlbaum, G.T. Wolff, Weekday/weekend ozone differences: what can we learn from them? J. Air Waste Manag. Assoc. 53 (2003) 772–788, https://doi.org/10.1080/10473289.2003.10466227.

[60] S. Zhou, C.J. Young, T.C. VandenBoer, T.F. Kahan, Role of location, season, occupant activity, and chemistry in indoor ozone and nitrogen oxide mixing ratios, Environ. Sci. Process. Impacts 21 (2019) 1374–1383, https://doi.org/10.1039/C9EM00129H.

[61] M. Othman, M.T. Latif, C.Z. Yee, L.K. Norshariffudin, A. Azhari, N.D.A. Halim, A. Alias, N.M. Sofwan, H.H.A. Hamid, Y. Matsumi, $PM_{2.5}$ and ozone in office environments and their potential impact on human health, Ecotoxicol. Environ. Saf. 194 (2020) 110432, https://doi.org/10.1016/J.ECOENV.2020.110432.

[62] K.K. Kalimeri, J.G. Bartzis, I.A. Sakellaris, E. de Oliveira Fernandes, Investigation of the $PM_{2.5}$, NO_2 and O_3 I/O ratios for office and school microenvironments, Environ. Res. 179 (2019) 108791, https://doi.org/10.1016/J.ENVRES.2019.108791.

[63] S. Schmitz, G. Villena, A. Caseiro, F. Meier, A. Kerschbaumer, E. von Schneidemesser, Calibrating low-cost sensors to measure vertical and horizontal gradients of NO_2 and O_3 pollution in three street canyons in Berlin, Atmos. Environ. 307 (2023) 119830, https://doi.org/10.1016/J.ATMOSENV.2023.119830.

[64] I. Christakis, G. Hloupis, I. Stavrakas, O. Tsakiridis, Low cost sensor implementation and evaluation for measuring NO_2 and O_3 pollutants, in: Proceedings of the 2020 9th International Conference on Modern Circuits and Systems Technologies, MOCAST, 2020, https://doi.org/10.1109/MOCAST49295.2020.9200245.

[65] N. Afshar-Mohajer, C. Zuidema, S. Sousan, L. Hallett, M. Tatum, A.M. Rule, G. Thomas, T.M. Peters, K. Koehler, Evaluation of low-cost electro-chemical sensors for environmental monitoring of ozone, nitrogen dioxide, and carbon monoxide, J. Occup. Environ. Hyg. 15 (2018) 87–98, https://doi.org/10.1080/15459624.2017.1388918.

[66] G. Bekö, P. Wargocki, N. Wang, M. Li, C.J. Weschler, G. Morrison, S. Langer, L. Ernle, D. Licina, S. Yang, N. Zannoni, J. Williams, The indoor chemical human emissions and reactivity (ICHEAR) project: overview of experimental methodology and preliminary results, Indoor Air 30 (2020) 1213–1228, https://doi.org/10.1111/ina.12687.

[67] A. Fischer, E. Ljungström, S. Langer, Ozone removal by occupants in a classroom, Atmos. Environ. 81 (2013) 11–17, https://doi.org/10.1016/j.atmosenv.2013.08.054.

[68] M. Zhang, J. Xiong, Y. Liu, P.K. Misztal, A.H. Goldstein, Physical–chemical coupling model for characterizing the reaction of ozone with squalene in realistic indoor environments, Environ. Sci. Technol. 55 (2021) 1690–1698, https://doi.org/10.1021/acs.est.0c06216.

[69] M.O. Fadeyi, C.J. Weschler, K.W. Tham, W.Y. Wu, Z.M. Sultan, Impact of human presence on secondary organic aerosols derived from ozone-initiated chemistry in a simulated office environment, Environ. Sci. Technol. 47 (2013) 3933–3941, https://doi.org/10.1021/es3050828.

[70] G. Morrison, A. Eftekhari, A. Fan, F. Majluf, J.E. Krechmer, The influence of personal care products on ozone-skin surface chemistry, PLoS One 17 (2022) e0268263, https://doi.org/10.1371/journal.pone.0268263.

[71] A.C. Rai, B. Guo, C.H. Lin, J. Zhang, J. Pei, Q. Chen, Ozone reaction with clothing and its initiated VOC emissions in an environmental chamber, Indoor Air 24 (2014) 49–58, https://doi.org/10.1111/INA.12058.